Effect of compression on fast swelling of poly(acrylamide-*co*-acrylic acid) superporous hydrogels

Richard A. Gemeinhart, Haesun Park, Kinam Park
Departments of Pharmaceutics and Biomedical Engineering, Purdue University, West Lafayette, Indiana 47907-1336

Received 6 June 2000; revised 19 September 2000; accepted 27 September 2000
Published online 4 January 2001

Abstract: Superporous hydrogels (SPHs) swell to a large size in a very short time. In many applications it is preferred to compress SPHs to reduce the overall dimension in the dried state. The effects of compression on the swelling property of SPHs were examined. The swelling property of the compressed SPHs was dependent on the orientation of the SPHs during compression. If SPHs were compressed in an orientated manner so that they retained interconnected porous structure, they were able to swell to near equilibrium within 10 min of immersion in aqueous fluids. If SPHs were compressed in a manner that did not retain the open pore structure, the swelling rate was greatly reduced. The results showed that the SPHs could be compressed without significant sacrifice of the fast swelling property if compressed in a proper orientation. Because pores were formed owing to the generation of gas which rose from bottom to the top of the container, the compression parallel to the pore formation resulted in preservation of the pore structure, and thus fast swelling property. The ability to compress SPHs, maintaining the fast swelling property, is expected to be useful in various applications including development of gastric retention devices for oral drug delivery. © 2001 John Wiley & Sons, Inc. J Biomed Mater Res 55: 54–62, 2001

Key words: superporous hydrogel; hydrogel; pore structure; compression; swelling

INTRODUCTION

Hydrogels have been used as an invaluable tool in the controlled drug delivery area.[1–3] The useful property of hydrogels in controlled drug delivery comes from slow swelling of dried hydrogels in water. The swelling of dried hydrogels results from diffusion of water through the glassy polymer causing disentanglement of polymer chains and subsequent swelling of the polymer network. This process is slow, which is why the dried hydrogels are used in controlled (i.e., slow) drug delivery. Although slow swelling of dried hydrogels is useful, there are situations where fast swelling and deswelling is desirable. For environment-sensitive hydrogels (also called smart hydrogels), fast changes in the swelling ratio would find wider applications.[4] For separation of biotechnology products, fast swelling and deswelling would be beneficial to save time for separation.[5] In our applications of hydrogels as a gastric retention device in oral drug delivery, we found that fast swelling in a matter of minutes was essential, and swelling of conventional hydrogels was too slow for the intended applications.[6] A novel comb-type of hydrogel was synthesized that possesses a fast shrinking property,[7] but such a hydrogel still did not have fast swelling property. For this reason, we developed superporous hydrogels (SPHs) that swell and shrink extremely fast.[8–11] Changes in the swelling ratio of the SPHs occur in a matter of minutes instead of hours by conventional hydrogels.

Whereas SPHs have high swelling ratios in the first place, compression of the SPHs in the dried state would provides additional means of increasing the swelling ratio. To achieve the highest swelling ratio possible, we investigated the possibility of compression of SPHs and its effect on the swelling kinetics. In our previous studies, we noticed that the pore shape within the SPH had a slight directionality, and it was hypothesized that the retention of the rapid swelling characteristics might be possible with proper compression techniques. By compression along the direction of the capillary network of the SPH, it was thought that the capillary channels in the SPH would be retained, allowing for rapid swelling. To confirm this hypothesis, we examined effects of compression along different directions of the synthesized SPHs.

Correspondence to: K. Park; e-mail: kpark@purdue.edu
Contract grant sponsor: NIH; Contract grant number: GM 08298

EXPERIMENTAL

Preparation of superporous hydrogels

All chemicals were from Aldrich Chemical Company (Milwaukee, WI) and used as received unless otherwise stated. SPHs were produced using acrylic acid and acrylamide with *N,N′*-methylene-*bis*-acrylamide (BIS) as the crosslinker in concentrations of 15% (v/v), 10% (w/v), and 0.25% (w/v), respectively. Pluronic® F127 (BASF Corporation, Parsippany, NJ) was added at a concentration of 0.5% (w/v). The redox initiator pair, *N,N,N′,N′*-tetramethylethylene diamine (TEMED) and ammonium persulfate (APS), was added at a concentration of 2% to the weight of monomer with TEMED being added to the stock monomer solution and APS added to the solution at the time of polymerization. Once the stock monomer solution was made, the pH of the solution was adjusted to 5.1 using 50% (w/v) sodium hydroxide. This solution was added to a 16 × 100-mm borosilicate culture tube (Fisher Scientific, Pittsburgh, PA) along with the appropriate amount of APS. Sodium bicarbonate (50 mg; Mallinkrodt Specialty Chemical Co, Paris, KY) was added 210 s after adding the initiators. The tube was then mixed thoroughly using a spatula to wet the sodium bicarbonate and to distribute the sodium bicarbonate evenly throughout the tube. Conventional hydrogels were also produced by substituting sodium bicarbonate with sodium hydroxide to the monomer mixture. Thus, the conventional hydrogels had the same composition as the SPHs but did not have any pores as in the SPHs. Polymerization was allowed to proceed for the next 4 h before the addition of absolute ethanol (McCormick Distilling Co., Brookfield, CT). Finally, the SPHs were dried in a food dehydrator (Mr. Coffee, Inc., Bedford Heights, OH) at a temperature of 80°C for 6 h.

Compression of superporous hydrogels

To compress the SPHs, it was necessary to have a plasticized polymer network. It was found that the SPHs had a rapid water uptake when placed at high humidity. The SPHs were placed in sealed chambers that contained salt solutions to maintain constant humidity. Three humidities were chosen for all of the experiments, 81%, 90%, and 99%. Samples were kept in the humidity chamber for prescribed times and removed. For some experiments, the weight of the SPH was taken before and after placement in the humidity chamber to determine water uptake in the humidity chambers. Percent weight increase (I) was calculated from the dry weight, w_d, and the plasticized weight, w_p, according to Equation (1).

$$I = [(w_p - w_d)/w_d]\ 100\% \quad (1)$$

The SPHs to be compressed were placed in a carver press and compressed with either a ¼-inch tablet punch and die or two stainless-steel plates. The tablet punch and die resulted in an axial compression, whereas two steel plates resulted in a radial compression. Figure 1 is a schematic representation of the compression process used. Two plates were used for the radial compression; a tablet punch and die were used for the axial compression. A laboratory Carver Press (Fred S. Carver Co., Menomonee, WI) was used for all of the compression experiments. The hand press was calibrated for pressures from 0 to 1000 lb. After removal from the press, the samples were immersed in absolute ethanol overnight. Samples were then dried in the food dehydrator and stored in a dessicator until use. The dimensions of the samples were measured using a digital micrometer (A. Daigger & Company, Lincolnshire, IL) before and after compression to determine the volume reduction after compression.

Mercury porosimetry

Pore size determination was conducted using an Autopore II 9220 (Micromeritics, Norcross, GA) mercury porosimeter. A 6-mL penetrometer was used for all experiments. The compressibility of the mercury, sample, and penetrometer were accounted for using standard procedures. For uncompressed SPHs, samples were taken from a 60°C oven and cut into 1-cm sections. Three samples from one SPH were considered a single data point. Because a pore volume of 0.39 mL was the maximum intrusion volume that could be measured, it was necessary to reduce the size of each piece for uncompressed SPHs. At least three samples were examined when the SPHs were cut, to take into account any error introduced by cutting the samples. Compressed SPHs were not cut and were examined in triplicate.

Samples were examined using two pressure regimens. The first pressure regimen was used for samples that were compressed. The second pressure regimen was used for the

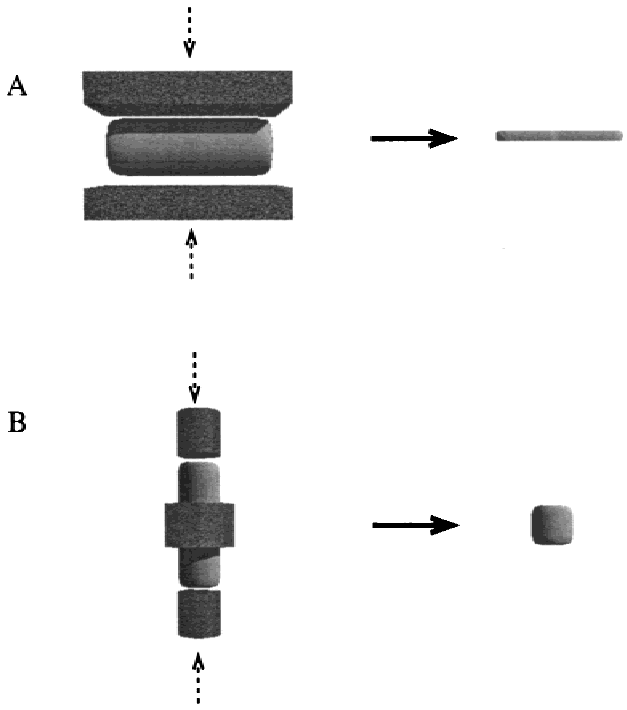

Figure 1. Schematic representation of the compression of SPHs. Radial (A) and axial (B) compression are shown. The compression of SPHs in the direction of the dotted arrows resulted in compressed SPHs in the shapes on the right.

uncompressed SPHs. It used more points at a lower pressure to more closely examine the exact pore size. From the Laplace equation, the diameter of the pores can be calculated when the contact angle and the surface tension of the intruding liquid are known for a given pressure. The contact angle was found to be 137.2 ± 0.6° using a goniometer (Ramé-Hart, Inc., Mountain Lake, NJ) and the surface tension, γ, of mercury was calculated to be 480 dyne/cm. The average pore diameter was determined from the graph of percent maximum intrusion volume versus the pore diameter. The density of samples was also calculated using mercury porosimetry. The samples with the known mass, m, were surrounded by a nonwetting fluid, mercury. From the weight of the mercury, the volume of the sample could be calculated before intrusion into the pores. The volume of the sample was determined at 0.5 psia, $V_{0.5\ \text{psia}}$, which was the lowest pressure at which no intrusion was assumed to take place. At high pressure, 60,000 psia, all pores were assumed to be filled with intruding mercury and the volume, $V_{60{,}000\ \text{psia}}$, of the sample was again determined. The density of the bulk material and the volume of the solid material were calculated from Equations (2) and (3), respectively.

$$\rho_{\text{bulk}} = m/V_{0.5\text{psia}} \tag{2}$$

$$\rho_{\text{solid}} = m/V_{60{,}000\text{psia}} \tag{3}$$

Scanning electron microscopy (SEM)

Scanning electron microscopy was used to determine the morphology of the dried samples. A JEOL JSM-840 scanning electron microscope (Jeol USA, Inc., Peabody, MA) was used after coating the samples with gold using a Hummer Sputter Coater (Technics, Ltd.). Images were captured using a digital capture card and Digital Scan Generator 1 (JEOL). Samples were cut using a scalpel to allow for the appropriate portion of the sample to be visible to the SEM. Samples were blown clean using compressed air (Envi-Ro-Tech™ Duster 1671; Tech Spray, Inc., Amarillo, TX), to remove any particles of the broken SPH.

Swelling studies

Swelling experiments were conducted using phosphate-buffered saline (PBS; pH ~ 7.4, I = 1.80). All data were obtained in triplicate. Samples were weighed and added to the PBS. At each time point from 15 s through 60 min, the sample was removed from the PBS. The sample was blotted dry with a Kimwipe® (Kimberly-Clark Corp., Roswell, GA) to remove excess water from the surface. Some water was still present in the pore structure and was considered to be part of the swollen network. Equation (4) was used to calculate the mass swelling ratio, Q, by using the dry weight, w_d, and the swollen weight, w_s.

$$Q = w_s/w_d \tag{4}$$

Compressive strength of superporous hydrogels

The SPHs were swollen in PBS as in the swelling studies. After at least 1 day in the solution and not more than 3 days, the SPHs were cut into pieces 2 cm in length. The diameter, d_s, of the swollen SPH was also recorded. Using a comparator (Ames, Waltham, MA), weight was applied to the SPH until the structure fractured and could support no more weight. The weight at fracture was recorded as the compressive strength of the SPH. Triplicate samples of each condition were examined. The mass, m, was converted to pressure (P) using Equation (5), where g is the acceleration due to gravity and A is the area of the SPH. This unit was chosen because it has been shown that the maximum pressure that the stomach exerts on an object during digestion is 7 kPa,[12] and we desired to show that the compressed SPHs retained the strength to withstand this pressure.

$$P = m\,g/A \tag{5}$$

RESULTS

Water uptake in humidity chambers

Water uptake patterns for the SPHs in three different humidity chambers over the first 6 h are shown in Figure 2. The water uptake at 81% and 90% relative humidity reached a plateau of 10% after 3 h of placement in the chamber. The water uptake at 99% relative humidity, however, continued to increase to more than 20% during the 7-h period. At early times, there was only a slight change in the plasticity of the SPHs, but at later times the SPHs became pliable and could easily be deformed. The overall size of the SPHs became noticeably smaller as time approached 5 h. By 6 h, the SPHs became so pliable that it was impossible to remove them from the humidity chamber without deforming the structure. For both the 81% and 90% humidity samples, similar results were found. The dif-

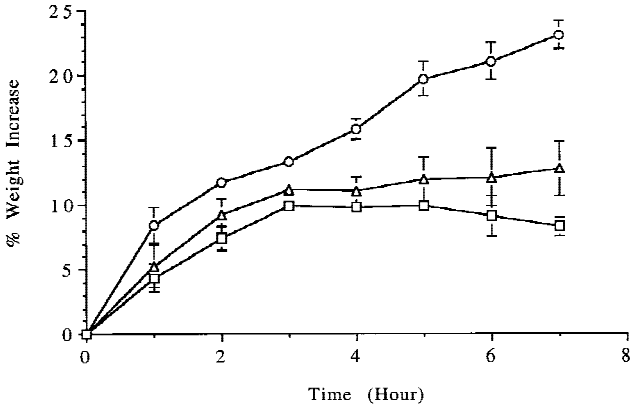

Figure 2. Percent water uptake over time for SPHs placed in 81% (□), 90% (△), and 99% (○) relative humidity chambers (n = 3).

ference between 90% and 81% was not statistically significant for early points and became significant as time passed. The difference in humidity between 90% and 99% was significant when considering the water uptake rate into the SPHs. On average, it took <2 h for the SPHs to reach a 10% weight increase in 99% humidity, whereas it took about 3 h in 81% and 90% humidities. When SPHs were kept at 99% humidity for long times (e.g., more than 3 h), swelling took place and the pore size began to expand, as described in Table I. The increase in size of the SPHs as a whole in Figure 2 confirmed that swelling took place as the dimensions of the superporous hydrogels changed and the weight began to increase significantly.

Effect of time spent in humidity chamber on compression

Samples were radially compressed at specific times after addition to the humidity chamber to determine the time of water uptake that was necessary for compression to take place. We found that there was some variation in the amount of time that it took for the SPHs to be sufficiently plasticized. Samples were removed every half hour after introduction into the humidity chamber. For samples at 99% humidity, the samples compressed at 30 min were crushed under 300 psia. At 60 min, two of the three SPHs could not be compressed, and at 90 min one SPH was crushed. Apparently, more time in the humidity chamber was required for effective compression. To show that the internal structure of the SPHs had not been compromised during compression, SPHs were compressed at 300 psia after 4 h in the 99% humidity chamber. The samples were swollen in PBS and the strength of the compressed SPHs was compared to the uncompressed SPHs. There was no statistical difference between the uncompressed and compressed (both radially and axially) samples (Fig. 3).

To determine the optimum amount of time that was needed in a humidity chamber and, hence, the optimum water uptake, SPHs were compressed radially every half hour after insertion into the humidity chambers. This was done for all three humidities used. Swelling and mercury porosimetry were used to characterize the samples as to the effect of time in the humidity chamber. The swelling of the SPHs for all humidities was a function of the time spent in the humidity chamber, and thus the percent water uptake. For the samples kept at 81% [Fig. 4(A)] and at 90% [Fig. 4(B)] humidity chambers, the swelling rate of the SPHs decreased as the amount of time spent in the humidity chamber increased up to 6 h. For the samples that were kept at 99% humidity before compression, the swelling rate initially decreased with time spent for plasticization; however, the swelling rate began to approach that of the uncompressed SPH after 330 and 360 min of plasticization [Fig. 4(C)]. That the swelling rate decreased as more plasticization occurred indicates that the SPHs were compressed more

TABLE I
Pore Diameter, Bulk Density, and Solid Density of SPHs Compressed after Plasticization at Different Relative Humidities

Sample		Pore Diameter (μm)	Bulk Density (g/mL)	Solid Density (g/mL)
Humidity (% RH)	Time (min)			
Hydrogel		0.01 ± 0.00	1.29 ± 0.02	1.33 ± 0.02
Uncompressed SPH		159.81 ± 21.57	0.30 ± 0.03	1.43 ± 0.15
81	180	22.97 ± 3.32*	0.89 ± 0.03	1.38 ± 0.04
81	240	21.84 ± 3.15*	0.94 ± 0.11	1.41 ± 0.02
81	300	7.37 ± 1.06	1.16 ± 0.01	1.47 ± 0.01
81	360	11.95 ± 1.73	1.09 ± 0.04	1.41 ± 0.01
90	150	36.76 ± 5.31†	0.71 ± 0.16	1.38 ± 0.01
90	210	28.58 ± 4.13†	0.82 ± 0.16	1.37 ± 0.02
90	270	13.57 ± 1.96‡	1.07 ± 0.08	1.20 ± 0.08
90	330	15.68 ± 2.26‡	1.04 ± 0.01	1.43 ± 0.01
99	120	35.61 ± 5.14§	0.50 ± 0.08	1.32 ± 0.08
99	180	24.65 ± 3.56‖	0.90 ± 0.07	1.36 ± 0.01
99	240	23.69 ± 3.42‖	1.01 ± 0.06	1.38 ± 0.00
99	300	46.14 ± 6.66§	0.69 ± 0.02	1.37 ± 0.01
99	360	65.17 ± 9.41	0.57 ± 0.07	1.39 ± 0.01

All samples were placed in an 81%, 91%, or 99% relative humidity chamber for the indicated amount of time, followed by compression at 300 psia. Immediately after compression, samples were placed in ethanol followed by drying in a food dehydrator ($n = 3$).

The symbols indicate the samples within a set of data that are not statistically different. The solid density of all of the samples was not statistically different ($p < .05$).

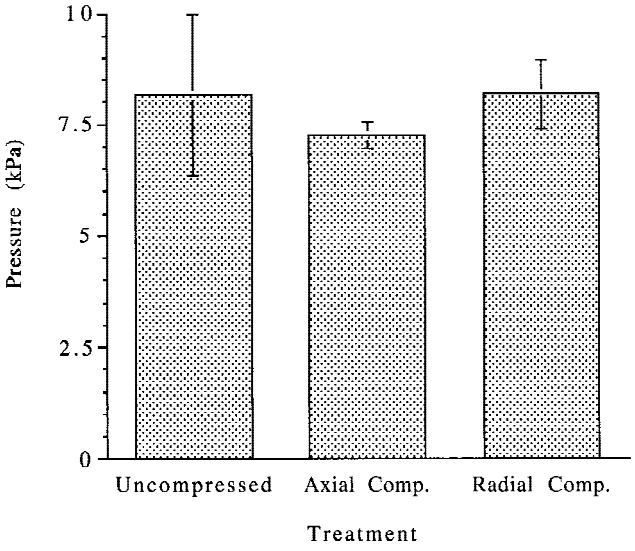

Figure 3. Compressive strength of the uncompressed and axially and radially compressed SPHs. All samples were kept at 99% humidity for 4 h before compression and immersed in ethanol after compression ($n = 3$).

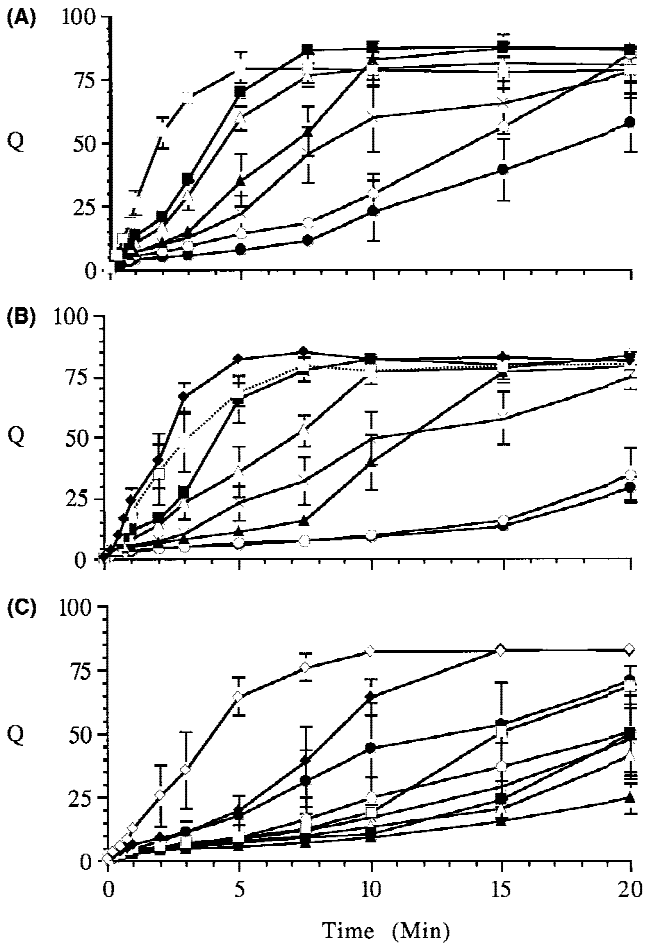

Figure 4. Swelling of the radially compressed SPHs as a function of the amount of time in the relative humidity chambers. The samples were kept at 81% (A), 90% (B), or 99% (C) humidity before compression at 300 psia for 30 s followed by immersion in ethanol (n = 3). In each humidity chamber, samples were kept for 120 min (◇), 150 min (◆), 180 min (□), 210 min (■), 240 min (△), 270 min (▲), 300 min (×), 330 min (○), and 360 min (●).

tightly with more plasticization. As shown in Table I, the pore size of the radially compressed SPHs decreased as time in the humidity chamber was extended with a slight increase at the final time point for those kept at 81% and those at 90%. This final increase in diameter was reproducible and was also seen with samples at the last two times for the SPHs kept at 99% humidity which also swelled at a rate slower than samples at shorter times in the humidity chamber. Thus, it appears that the slow swelling of the SPHs kept in the humidity chambers longer is due to the tighter compression of the SPHs, leading to partial blockage of the interconnected pores. When the water uptake by SPHs in the humidity chamber was small, i.e., approximately 10%, the density of the radially compressed SPHs was greater than the bulk density of the uncompressed SPH, 0.30 ± 0.03 g/mL. At 180 and 240 min in an 81% humidity chamber, the bulk density of the radially compressed SPHs was approximately 0.90 g/mL. This was also the value of the samples compressed after being kept in the 90% humidity chamber for 150 and 210 min.

Comparison of Figures 2 and 4 and Table I indicates that weight increase of about 10% by water uptake appears to be the optimum condition for compression. The larger uptake of water may make the SPHs too pliable during compression, leading to extensive compaction of polymer chains. The optimum bulk densities of the SPHs for compression without a substantial sacrifice in swelling property, however, was different depending on the humidity used. For the SPHs kept at 81% humidity, those with the bulk density <0.94 ± 0.11 g/mL resulted in satisfactory compression and swelling to equilibrium in <10 min. The optimum bulk density value decreased to 0.82 ± 0.16 and 0.50 ± 0.08 g/mL for those kept at 90% and 99% humidities, respectively. The data collectively suggest that it is better to plasticize by incubating at a low humidity (e.g., 81%) for a longer period of time than at a high humidity for a shorter period of time, even if both conditions resulted in the same amount of water uptake.

Effect of compression pressure

We observed that the pressure used to compress SPHs influenced the thickness of the compressed SPHs. For this reason, we investigated the thickness of the SPHs to determine the optimum pressure for the reduction in size of the SPH while retaining the speed of swelling. We found that the thickness of the radially compressed SPHs was inversely related to the pressure used to compress the SPH (Table II). The thickness of an uncompressed SPH was 8.71 ± 0.40 mm. Because the width and length of the samples did not change appreciably after compression, the volume reduction of the samples was only related to the reduction in thickness of the compressed SPHs. The diam-

TABLE II
Thickness and Volume Reduction for Radially Compressed SPHs

Pressure (lb)	Thickness (mm)	% SPH Volume
Uncompressed	8.71 ± 0.40	100
200	1.88 ± 0.11*	27
400	1.73 ± 0.10*	25
600	1.41 ± 0.03†	21
800	1.32 ± 0.10†‡	19
1000	1.14 ± 0.04‡	17

The samples were kept at 99% humidity for 2 h before compression for 30 s. The samples were then immersed in ethanol.

The symbols indicate the samples within a set of data that are not statistically different. The solid density of all of the samples was not statistically different (p < .05) (n = 3).

eter of the sample was the thickness and width of the uncompressed SPH. The reduction in volume of the SPH after compression ranged from 17% to 27%. This means that the overall swelling ratio can be increased by a factor ranging from 3.7 to 5.9. Thus, SPHs which have the intrinsic swelling ratio of 100 would have the overall swelling ratios of 370 ~ 590. This is especially useful because there was only a small difference in the swelling characteristics for the SPHs compressed at different pressures (Fig. 5). In Figure 5, 0 psia pressure was applied by stopping compression at the point where the press showed the first sign of registering pressure. The time for full swelling in Figure 5 ranged from 2 to 10 min, but the important point is that all of them swelled to equilibrium within 10 min, which is still orders of magnitude higher than the swelling of conventional hydrogels of the same sizes. The lack of significant differences in the swelling of the SPHs was also seen in the data from mercury porosimetry (Table III). The pore diameter ranged from 15 to 34 μm without statistical differences. The density and pore volumes also remained the same for all pressures.

TABLE III
Pore Diameter, Bulk Density, and Solid Density of Radially Compressed SPHs Measured by Mercury Porosimetry

Sample	Pore Diameter (μm)	Bulk Density (g/mL)	Solid Density (g/mL)*
Hydrogel	0.01 ± 0.00†	1.29 ± 0.02†	1.33 ± 0.02
Uncompressed SPH	159.81 ± 21.57‡	0.30 ± 0.03‡	1.43 ± 0.09
0 psia	124.78 ± 30.00‡	0.43 ± 0.15‡	1.41 ± 0.21
200 psia	33.58 ± 8.43†	0.90 ± 0.15†	1.56 ± 0.07
300 psia	17.04 ± 10.06†	1.03 ± 0.02†	1.43 ± 0.02
400 psia	15.64 ± 8.86†	1.06 ± 0.04†	1.42 ± 0.01
600 psia	26.43 ± 5.39†	0.95 ± 0.10†	1.43 ± 0.01
800 psia	27.10 ± 6.76†	0.97 ± 0.05†	1.37 ± 0.05
1000 psia	20.02 ± 10.57†	1.07 ± 0.10†	1.46 ± 0.03

All samples were placed in a 99% relative humidity chamber for 2 h followed by compression, as indicated. Immediately after compression, samples were placed in ethanol followed by drying in a food dehydrator (n = 3).

The symbols indicate the samples within a set of data that are not statistically different.

*The solid density of all samples is not statistically different (p < .05).

Effect of direction of compression

Swelling kinetics of the samples compressed axially and radially were different. As shown in Figure 5, all of the radially compressed SPHs swelled to equilibrium values within 10 min regardless of the compression pressure used. On the other hand, axially compressed SPHs swelled at a rate much slower than that of the uncompressed and radially compressed SPHs (Fig. 6). Even after 20 min, the swelling ratio of the axially compressed SPHs was <5, whereas that of uncompressed and radially compressed SPHs was ~70. There was a point at approximately 30 min at which the axially compressed SPHs swelled quickly. This point was highly variable and could not be reproduced despite repeated attempts. The variability ranged from 30 min to 2 h. The conditions for controlling the exact time of swelling of the axially compressed SPH, if any, were not discovered. It is believed that at the time at which the pore structure of the SPH opens, the SPH swells suddenly. This, however, needs to be confirmed.

From the scanning electron micrographs (Fig. 7) it can be seen that the pores in the compressed SPHs were closed during axial compression. The porous structure interior of the SPH [Fig. 7(A)] was nearly closed after compression. The pore size was only 2.61 ± 2.11 μm (Table IV). The image from the top of the compressed SPH [Fig. 7(B)] also showed little poros-

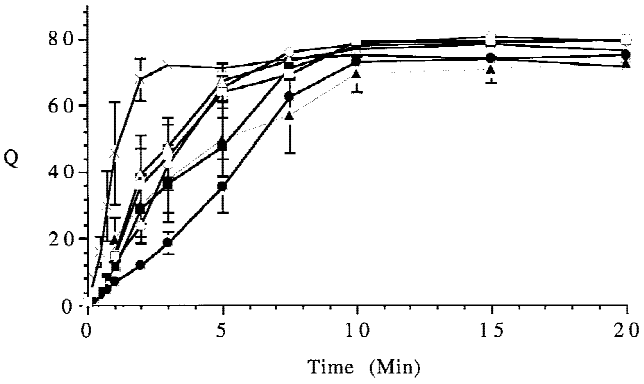

Figure 5. Swelling of radially SPHs compressed radially at various pressures. The SPHs were kept at 99% humidity for 2 h before compression. After compression, the SPHs were immersed in ethanol (n = 3). Pressure applied were 0 psia (□), 200 psia (■), 400 psia (○), 600 psia (●), 800 psia (△), 1000 psia (▲), and no compression (×).

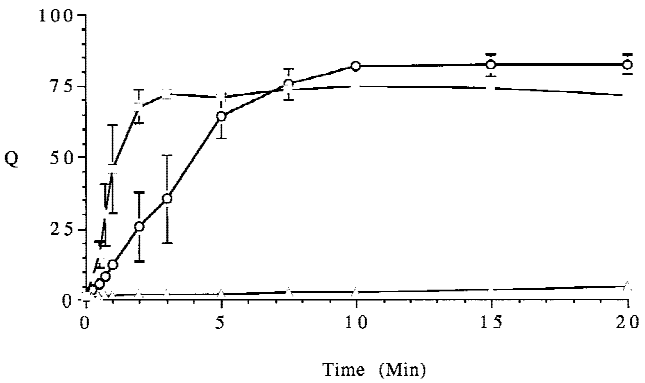

Figure 6. Swelling of uncompressed (□), radially compressed (○), and axially compressed (△) SPHs. All samples were kept at 99% humidity for 120 min before compression and immersed in ethanol after compression (n = 3).

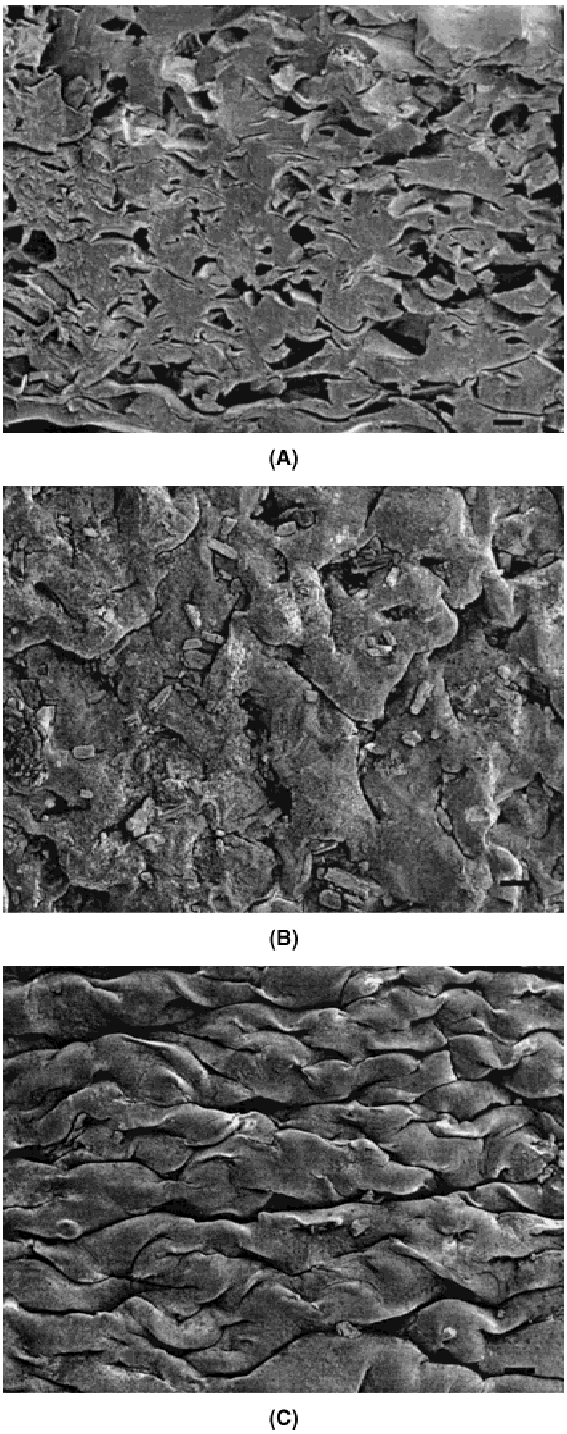

Figure 7. Scanning electron micrographs of the interior (A), top (B), and side (C) of an axially compressed SPH. The images were taken at a magnification of ×50, and the scale bar is 100 μm.

ity, and the side image [Fig. 7(C)] showed a folded structure due to compression. All images showed the lack of connectivity among pores. For the radially compressed SPHs, however, the interior structure was relatively highly porous and most of the pores were interconnected [Fig. 8(A)], although the average pore diameter (17.04 ± 11.86 μm) was still much smaller than that of the uncompressed SPH (159.81 ± 21.57 μm). The exterior structure of radially compressed SPHs [Fig. 8(B)] was similar to the uncompressed SPH. The bulk densities of the compressed SPHs were almost equivalent to the bulk and solid density of a conventional hydrogel (Table IV), whereas the solid densities of all of the SPHs were equivalent to the conventional hydrogel. The bulk densities of the axially and radially compressed SPHs were 1.13 ± 0.07 and 1.03 ± 0.05, respectively, which were statistically the same. This means that the volumes of the axially and radially compressed SPHs were actually the same. Thus, the difference in swelling rate between radially and axially compressed SPHs in Figure 6 is most likely due to the changes in pore structures by different orientations for compression.

DISCUSSION

The water uptake and plasticization found at high humidity were expected. Shrinkage of the SPHs during plasticization, however, was unexpected. Water is a good solvent for the SPH polymers (made of acrylic acid and acrylamide), and thus the water vapor is expected to have a fast diffusion through the polymer network.[13] The shrinking of the SPHs when placed at high humidity may be due to relaxation of the polymers as they are becoming plasticized and cross their glass transition. Because the polymers were dried in a nonsolvent, ethanol, they were not allowed to relax during the drying process. As the polymer chains become wet, they are allowed to rearrange to be in their most thermodynamically favored state. The chains will be denser than the original state owing to the smaller amount of hydration present in the system compared with the polymer before addition of nonsolvent and the sample in the humidity chamber. For samples that are air dried or dried in gradients of ethanol, the size of the air-dried samples was much smaller than the ethanol-dried samples, confirming the idea that the ethanol may lock the polymer structure in a less thermodynamically favored state. The fact that the polymer chains were locked into this state may also contribute to the speed of swelling, because of a reduced need for the polymer chains to rearrange during swelling. This is because there is less rearrangement of the polymer chains and possibly larger areas for diffusion in the dried polymers.

In plasticization of SPHs using water, the weight gain of the SPHs showed good correlation with the plasticization of the SPHs. All SPHs that had not increased in weight by at least 10% were not compressible. Slightly below the 10% water uptake, at first some SPHs looked compressible, but cracking of the struc-

TABLE IV
Pore Diameter, Bulk Density, and Solid Density of Uncompressed, Axially Compressed, and Radially Compressed SPHs

Sample	Pore Diameter (μm)	Bulk Density (g/mL)	Solid Density (g/mL)*
Hydrogel	0.01 ± 0.00†	1.29 ± 0.02†	1.33 ± 0.02
Uncompressed SPH	159.81 ± 21.57	0.30 ± 0.03	1.43 ± 0.09
Axially compressed SPH	2.61 ± 2.11†	1.13 ± 0.07†‡	1.40 ± 0.01
Radially compressed SPH	17.04 ± 11.86†	1.03 ± 0.05‡	1.43 ± 0.01

All samples were placed in a 99% relative humidity chamber for 2 h followed by appropriate compression at 300 psia. Immediately after compression, samples were placed in ethanol followed by drying in a food dehydrator (n = 3).
The symbols indicate the samples within a set of data that are not statistically different.
*The solid density of all samples was not statistically different.

ture had taken place. Some of the cracks were so hidden that they were not noticeable until they were swollen, when pieces of these SPHs broke off during swelling. For SPHs that had reached at least 10% water uptake, there was no evidence of cracking in the samples from SEM or mechanical studies.

The radially compressed SPHs kept at 99% humidity showed the most dramatic variation in density (Table I). This is due to the amount of plasticization that had taken place. For the 81% and 90% humidity samples, there was not sufficient time for the uptake of enough water to become fully plasticized. The samples left in the 99% humidity chamber had enough moisture present that when they were immersed in ethanol, the polymer chains were not immediately dehydrated. The samples began to decompress and had regions that were almost half the thickness they had had before compressing. This decompression was the reason for the larger pore size, decreased density, and increased pore volume of samples that were kept at 99% humidity for >300 min. This also explained the rapid swelling for the samples kept at 99% humidity for the longest times. There was sufficient pore volume and pore diameter for the swelling of the SPHs because the SPHs had too much water present to stay compressed. Samples kept at lower humidities showed the same decompression phenomena when the time at the specific humidity was long enough. As long as the plasticization was controlled, the properties of the compressed SPH could be well controlled.

The radially compressed samples did not swell at the same rate as the uncompressed SPHs; however, they did swell within 10 min of immersion into PBS. If the SPHs are to be used as an effective gastric retention device, it is thought that the device must swell before the interdigestive migrating myoelectric complex (IMMC). This takes place after the last digestible contents are removed from the stomach. Normal digestive contractions take place until the last liquid contents of the stomach are removed. After this time, the basal period of the IMMC begins and lasts between 45 and 60 min.[14] The SPH should be swollen before the end of the basal period if the gastric retention device is to succeed. Because even the (radially) compressed SPHs swelled to semiequilibrium in 10 min, there should be sufficient time for the compressed SPHs to swell in the stomach if a sufficient amount of water is administered in the beginning.

In summary, the SPHs may become more useful by reducing their volume. It took <2 h in a 99% humidity chamber for the SPH to be compressible, and only 300 psia was needed to have reproducible compressed SPHs. One must consider, however, that the SPH

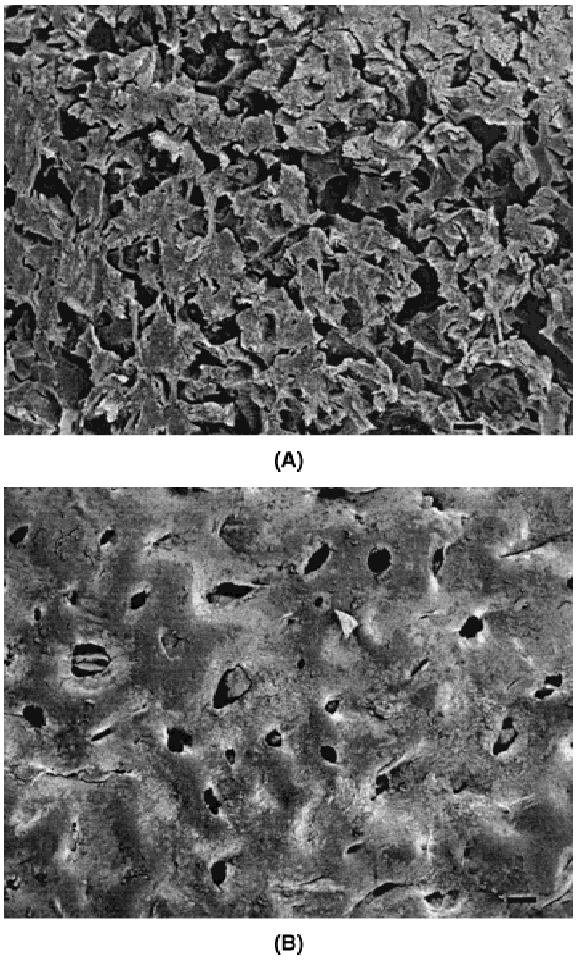

Figure 8. Scanning electron micrographs of the interior (A) and side (B) of a radially compressed SPH. The images were taken at a magnification of ×50, and the scale bar is 100 μm.

needs to be compressed to maintain the pore structure intact. If the pore structure of the compressed SPHs is disturbed, the swelling rate will be much too slow to be useful. Compression to the direction parallel to the formation of pores can maintain open pore structures necessary for fast swelling.

The authors thank Debra Sherman, at the Microscopy Center in Agriculture, for assistance with and use of the scanning electron microscope.

References

1. Peppas NA. Hydrogels in medicine and pharmacy, vol. I–III. Boca Raton, FL: CRC Press, 1987.
2. Park K, Shalaby SW, Park H. Biodegradable hydrogels for drug delivery. Lancaster, PA: Technomic Publishing, 1993. p 1–12.
3. Miyata T, Asami N, Uragami T. Reversibly antigen-responsive hydrogel. Nature 1999;399:766–769.
4. Park K, Park H. Smart hydrogels. In: Salamone JC, editor. Concise polymeric materials encyclopedia. Boca Raton, FL: CRC Press, 1999. p 1476–1478.
5. Kim JJ, Park K. Applications of smart hydrogels in separation. In: Mattiasson B, Galaev I, editors. Smart polymers for bioseparation and bioprocessing. Amsterdam, The Netherlands: Harwood Publishers (to appear).
6. Shalaby WS, Blevins WE, Park K. *In vitro* and *in vivo* studies of enzyme-digestible hydrogels for oral drug delivery. J Control Rel 1992;19:131–144.
7. Yoshida R, Uchida K, Kaneko Y, Sakai K, Kikuchi A, Sakurai Y, Okano T. Comb-type grafted hydrogels with rapid de-swelling response to temperature changes. Nature 1995;374:240–242.
8. Chen J, Park H, Park K. Synthesis of superporous hydrogels: Hydrogels with fast swelling and superabsorbent properties. J Biomed Mater Res 1999;44:53–62.
9. Chen J, Park K. Superporous hydrogels: Fast responsive hydrogel systems. JMS Pure Appl Chem 1999;A36:917–930.
10. Chen J, Park K. Synthesis of fast-swelling, superporous sucrose hydrogels. Carbohydrate Polymers 2000;41:259–268.
11. Chen J, Blevins WE, Park H, Park K. Gastric retention properties of superporous hydrogel composites. J Control Rel 1999; 64:39–51.
12. Guyton AC. Basic human physiology: Normal function and mechanisms of disease. 2. Philadelphia, PA: WB Saunders, 1977. p 662–664.
13. Flory PJ. Principles of polymer chemistry. Ithaca, NY: Cornell University Press, 1953. p 576.
14. Kelly KA. Motility of the stomach and gastroduodenal junction. In: Johnson LR, editor. Physiology of the gastrointestinal tract. New York: Raven Press, 1981. p 393–410.